CARBON 62 (2013) 193–203

Available at www.sciencedirect.com

SciVerse ScienceDirect

journal homepage: www.elsevier.com/locate/carbon

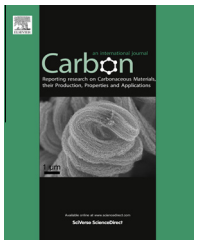

Surface modification of nanocast ordered mesoporous carbons through a wet oxidation method

A. Sánchez-Sánchez *, *F. Suárez-García*, *A. Martínez-Alonso*, *J.M.D. Tascón*

Instituto Nacional del Carbón, INCAR-CSIC, Apartado 73, 33080 Oviedo, Spain

ARTICLE INFO

Article history:
Received 22 April 2013
Accepted 5 June 2013
Available online 13 June 2013

ABSTRACT

An ordered mesoporous carbon was synthesized by chemical vapor deposition using SBA-15 silica as solid template and propylene as carbon precursor. It was submitted to several liquid oxidation treatments by means of HNO_3 and H_2O_2 under different oxidation conditions in order to modify its surface chemistry while keeping its structure and porous texture as unmodified as possible. Original and modified OMC samples were characterized using different techniques such as nitrogen adsorption at - 196 °C , X-ray diffraction, scanning electron microscopy, elemental analysis, temperature programmed desorption and X-ray photoelectron spectroscopy. A higher amount of oxygen functional groups was introduced on the material surface by using HNO_3 than by means of H_2O_2, but the original surface texture and structural arrangement were kept unchanged in both cases.

1. Introduction

Ordered mesoporous carbons (OMCs) synthesized by nanocasting method have received increasing attention in recent years because of their excellent properties such as high surface areas and pore volumes, uniform and narrow pore size distributions, high thermal stability and good electric conductivity. All these properties make them suitable materials for their application as sensors, adsorbents, catalyst supports, electrode materials or energy storage systems [1]. To this end, mesoporous silicas with variable pore size and structure have been extensively infiltrated with suitable carbon precursors via a liquid infiltration method [2] or chemical vapor deposition (CVD) [3,4]. Subsequent carbonization and removal of silica template, using HF or NaOH solutions, give rise to different OMCs that preserve the original templates' morphology and constitute inverse replicas of them. These materials contain, in general, a small amount of functional groups (i.e. oxygen-containing groups) on their surface, which could be a clear limitation, both for many applications (where functional groups are needed for developing specific interactions) [5] and for grafting their surface with other functional groups, where oxygen-containing surface groups act as anchors [6].

The introduction of oxygen-containing functional groups on the carbon surface can be attained by means of oxidation post-treatments [6–8]. Thus, oxidation treatments (typically dry, wet, plasma or electrochemical oxidation) have been frequently used because they can introduce a large amount of oxygen functional groups on the carbon surface. The behavior of the oxidizing agents generally differs with regard to the quantity and predominant type of functional groups that they introduce, and it has been widely reported that nitric acid oxidation is the most effective one in terms of surface chemistry modification of carbon materials [9]. Therefore, it is important not only to introduce a certain amount of surface functional groups (especially carbon–oxygen complexes) under specific experimental conditions, but also to indentify the nature of the functional groups generated. The functionalization of

* *Corresponding author:* Fax: +34 985 297 662.
E-mail address: ang.san@incar.csic.es (A. Sánchez-Sánchez).
0008-6223/$ - see front matter
http://dx.doi.org/10.1016/j.carbon.2013.06.011

OMCs has to be carried out carefully in order to prevent the structural collapse of their ordered framework. Different works on the oxidation/functionalization of OMCs such as CMK-3 and CMK-5 can be found in the literature [6,9–16]. In general, it was concluded that CMK-3 maintains the structural order to a large extent, while the CMK-5 structure was more sensitive and a collapse easily occurred. This is due to the differences in the 3D structure of both materials, composed of interconnected carbon rods in CMK-3 carbon and interconnected carbon pipes in CMK-5, the latter being more prone to collapse.

The aforementioned OMCs were mostly obtained via liquid impregnation using different carbon precursors [1,2,4,10–13,17–20], and only a few works have dealt with the oxidation of OMCs obtained by the CVD method [21]. In this work, a CMK-3 type OMC obtained from CVD of propylene was subjected to different liquid phase oxidation treatments using both nitric acid and hydrogen peroxide, in order to introduce an as high as possible amount of surface oxygen functional groups without disturbing the original ordered mesoporous structure. This work focuses on performing a systematic study of the surface chemistry evolution of CVD-synthesized CMK-3 carbon as a function of oxidant nature, concentration and oxidation time.

2. Experimental

2.1. Synthesis of SBA-15 template

Mesoporous SBA-15 silica was prepared by a soft-templating method using a triblock copolymer (Pluronic P123, Mw = 5800, Sigma–Aldrich) as synthesis directing agent, and TEOS (Sigma–Aldrich) as silica source, as described by Zhao et al. [22]. Typically, 10.44 g P123 was added to an aqueous solution containing 52.5 mL of 37% HCl (Merck), and stirred at 40 °C. Once the dissolution of the triblock copolymer was complete, 22.64 g 98% TEOS was added dropwise, stirring the mixture at the same temperature for 4 h. The resulting product was aged at 125 °C for 72 h, filtered and calcined in air at 550 °C during 6 h.

2.2. Synthesis of ordered mesoporous carbon

OMC was obtained following a hard-templating method via a chemical vapor deposition route, as reported elsewhere [19,23]. The calcined SBA-15 was placed in a flow-through tube furnace and heated to 750 °C under an argon flow (99.999% purity) with a heating ramp of 10 °C/min, and then maintained at this temperature for 6 h under a propylene flow (99.5% purity). Subsequent carbonization was carried out at 900 °C with a heating ramp of 5 °C/min under an argon flow. The resulting silica–carbon composite was treated with 48% HF (*Merck, Normapur*) at room temperature in order to remove the silica template, filtered and washed several times with distilled water, and dried at 80 °C. The obtained OMC was designated as X1.

2.3. Wet oxidation of ordered mesoporous carbon

The surface chemistry of mesoporous carbon X1 was modified by means of several treatments of different strength in liquid phase. Typically, 1 g dried X1 carbon was oxidized under mild conditions with 150 mL of (a) 30% (v/v) H_2O_2 (*Merck, Emsure ISO for analysis*) at ambient temperature for 4 or 24 h (named here as X1ox4A and X1ox24A, respectively); and (b) 0.5 M HNO_3 (*solution from commercial concentrated product, Sigma–Aldrich*) heating at 80 °C for 1–5 h. More severe oxidation conditions were applied using 150 mL of (c) 2 M and (d) 5 M HNO_3 (*solutions from commercial concentrated product, Sigma–Aldrich*), heating at 80 °C, from 1 to 5 h in the first case and from 3 to 5 h in the second one (carbons oxidized with HNO_3 at 80 °C were denoted as X1oxB/C, where B corresponds to the HNO_3 molarity used and C is the treatment duration in hours), and (e) 14.55 M HNO_3 (*Sigma Aldrich, commercial concentrated product*), at room temperature during 1 h (named X1oxC/1).

2.4. Characterization techniques

The porous texture of the samples was characterized through N_2 adsorption/desorption isotherms at - 196 °C using an Autosorb-1 (Quantachrome) volumetric adsorption apparatus. Porous texture parameters obtained from these isotherms were: the apparent BET surface area, S_{BET}, calculated through BET method; the total pore volume, V_t, calculated from the amount adsorbed in liquid form at $P/P_0 = 0.975$; the micropore volume, V_{micro}, calculated by applying the Dubinin–Radushkevich equation; and the mesopore volume, V_{meso}, calculated as the difference between V_t and V_{micro}. The pore size distributions (PSDs) were obtained by applying the quenched solid density functional theory method (QSDFT). The main pore size, *D*, was determined from these PSDs at the maximum value. Structural and morphological characterizations were carried out by X-ray diffraction and scanning electron microscopy, with a Siemens D5000 diffractometer (Cu K_α radiation; scanning range $2\theta = 0.5$-5°; step width = 0.01°; time per step = 1 second) and a Carl Zeiss DMS-942 microscope, respectively. Finally, chemical characterization was performed by elemental analysis using a LECO CHNS-932 microanalyzer and a LECO VTF-900 microanalyzer for oxygen; X-ray photoelectron spectroscopy was carried out on a SPECS system, working at a pressure of 10^{-7} Pa with a monochromatic Al K_α X-ray source (1486.3 eV, 150 W). The photo-excited electrons were analyzed in constant pass energy mode, using a pass energy of 30 eV for the survey spectra and 10 eV for the high resolution core level spectra. The CasaXPS software was used for data processing and all envelopes of core level spectra were peak-fitted with a Gaussian–Lorentzian convoluted function (80/20) and a Shirley's background. The compositions (in wt.%) were determined from the survey spectra by considering the integrated peak areas of the main XPS peaks of the different elements (C1s and O1s) and their respective sensitivity factors. Temperature programmed desorption (TPD profiles) was carried out with an Autochem II apparatus (Micromeritics). The samples were heated at a constant rate of 10 °C/min to 1000 °C under a He flow of 50 mL/min, and the evolved gases (CO and CO_2) were monitored using an Omnistar (Pfeiffer Vacuum) mass spectrometer. The amounts of released CO and CO_2 were determined from the intensities of *m*/*z* at 28 and 44, respectively.

3. Results and discussion

Nitrogen adsorption isotherms at -196 °C of original and a selection of the oxidized carbons are shown in Fig. 1A, and several textural parameters are collected in Table 1.

As we can see in Fig. 1A, both the pristine and the oxidized OMCs exhibit type IV isotherms (according to IUPAC classification), typical of mesoporous materials. Nitric acid oxidation does not apparently modify the porous texture of X1 OMC. Thus, all samples show almost the same isotherms and PSDs (see Fig. 1B) as the original carbon. In the case of H_2O_2 oxidation, the isotherm is close to that for the original carbon at low and medium P/P_0, but at high relative pressures larger N_2 uptakes are observed, which implies the presence of a greater amount of large mesoporous in the oxidized carbon (around 10 nm in size, as it can be observed in the corresponding PSD shown in Fig. 1B). This indicates that H_2O_2 has a slightly higher capacity to remove carbon atoms from the X1 surface than HNO_3. The ability of H_2O_2 for cleaving C–C bonds through oxidative degradation with the formation of small organic molecules has been demonstrated in the case of CMK-5 type carbons [13].

Despite this, the PSDs are clearly maintained after both mild and strong oxidation treatments as can be noticed in Fig. 1B. The main pore size, *D*, does not change following the post-treatments (see Table 1). As can be expected from Fig. 1A and B, textural parameters listed in Table 1 virtually do not differ between the oxidized carbons and the starting material. This suggests that, unlike other works, no introduction of oxygen functional groups that can partially block the porosity takes place. Only in the case of samples oxidized with H_2O_2, higher V_t and V_{meso} are observed, probably due to collapse of adjacent mesopores during the oxidation process by rupture of the walls that separate them. These results indicate that the porous texture of samples is unaffected after oxidation treatments with HNO_3 and only some large mesopores are produced by H_2O_2 treatments, but even in this case the main pore structure is preserved.

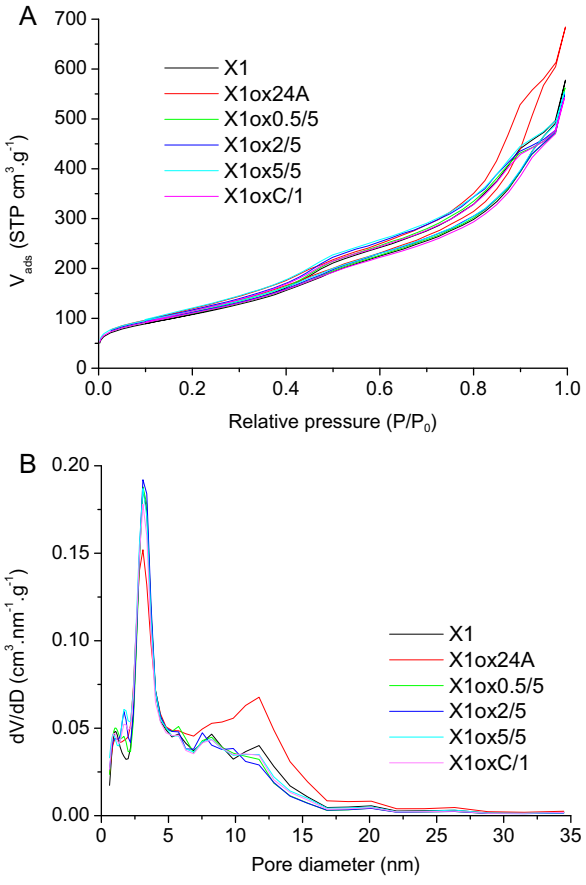

Fig. 1 – (A) Nitrogen adsorption isotherms at - 196 °C and (B) pore size distributions of raw and several oxidized carbon materials.

As concerns the structure of both oxidized and raw OMCs, the X-ray diffraction profiles (Fig. 2) show in all materials well-resolved (100), (110) and (200) peaks, corresponding to a two-dimensional hexagonal arrangement, even in the samples that were submitted to the most severe oxidation conditions. This arrangement consists of carbon rods templated from the mesoporous network of silica, plus carbon connectors originated from templating of silica wall micropores. The higher intensity of the (100) reflection in respect to that for the (110) reflection indicates that X1 sample has a CMK-3 type structure formed by carbon rods (as evidenced also by TEM, see Fig. S1 in Supporting Information) and not by carbon pipes (CMK-5 structure), which would yield a higher intensity of the (110) peak regarding the (100) peak [16]. Values of the interplanar distance, $d_{(100)}$, the unit cell parameter, *a*, and the diameter of carbon rods, *E*, are listed in Table 1. The unit cell parameter corresponding to a two-dimensional hexagonal arrangement was calculated through equation, $a = 2/(3)^{1/2}$. $d_{(100)}$, and the diameter of the carbon rods was calculated by means of $E = a - D$[24,25], where $d_{(10\,0)}$ is the interplanar distance obtained from Bragg's law and *D* is the pore diameter obtained at the maximum value of the PSDs.

As shown in Table 1, the oxidized carbons present insignificant variations in both the unit cell parameter (*a*) and the diameter of carbon rods (*E*) with respect to the raw OMC. This fact, and the presence of well-resolved peaks in the oxidized materials, indicates that oxidation treatments do not alter the two-dimensional hexagonal structure of the raw carbon.

Scanning electron micrographs of the original ordered mesoporous carbon, X1, and samples obtained from several oxidation treatments are recorded in Fig. 3.

Comparing the original carbon (Fig. 3A) with those obtained through oxidation with 5 M HNO_3/80 °C/5 h (X1ox5/5) (Fig. 3C) and H_2O_2/room temperature/24 h (X1ox24A) (Fig. 3B), no changes in particle structure can be observed following the oxidative treatments. However, the carbon treated with concentrated HNO_3/room temperature/1 h (Fig. 3D) presents isolated and scarce damaged areas, consisting in localized collapses of the structure, which generally do not alter the properties regarding the starting material. In fact, Fig. 3D shows a selected local collapse, but the overall morphology of this carbon presents similar textural and crystallographic parameters to the rest of carbons.

The results related to textural, structural and morphological characteristics of modified materials discussed thus far indicate that after oxidation treatments, under either mild

Table 1 – Textural and structural parameters obtained from nitrogen adsorption isotherms at - 196 °C and X-ray diffraction techniques, respectively.

Sample	Nitrogen adsorption isotherms at - 196 °C					XRD		
	S_{BET} ($m^2\ g^{-1}$)	V_t ($cm^3\ g^{-1}$)	V_{micro} ($cm^3\ g^{-1}$)	V_{meso} ($cm^3\ g^{-1}$)	D (nm)	$d_{(100)}$ (nm)	a (nm)	E (nm)
X1	406	0.76	0.14	0.62	3.1	10.1	11.7	8.6
X1ox4A	428	0.88	0.14	0.74	3.1	10.2	11.8	8.7
X1ox24A	401	0.85	0.15	0.70	3.1	9.9	11.4	8.3
X1ox0.5/1	393	0.72	0.15	0.57	3.1	10.1	11.7	8.6
X1ox0.5/3	396	0.74	0.15	0.59	3.1	10.2	11.8	8.7
X1ox0.5/5	413	0.73	0.16	0.57	3.1	10.2	11.8	8.7
X1ox2/1	396	0.72	0.15	0.57	3.1	10.0	11.5	8.4
X1ox2/3	410	0.73	0.16	0.57	3.1	10.1	11.7	8.6
X1ox2/5	417	0.73	0.16	0.57	3.1	10.2	11.8	8.7
X1ox5/3	440	0.77	0.14	0.63	3.1	10.1	11.7	8.6
X1ox5/5	427	0.76	0.15	0.61	3.1	10.1	11.7	8.6
X1oxC/1	415	0.73	0.15	0.58	3.1	10.1	11.7	8.6

d_{100}, Interplanar distance, obtained by means of Bragg's law; a, unit cell parameter, calculated as $2/(3)^{1/2}d_{(100)}$; E = diameter of carbon rods, calculated as the difference between the unit cell parameter (a) and the pore diameter (D).

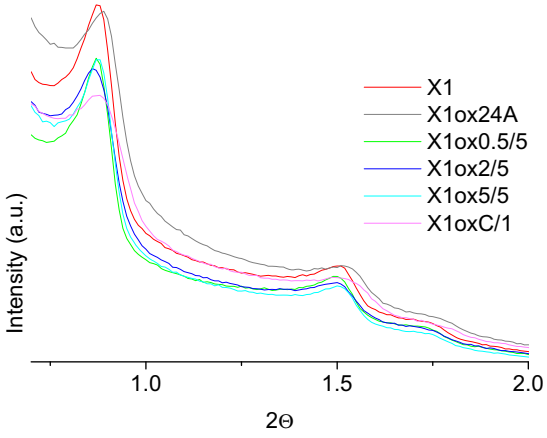

Fig. 2 – X-ray diffraction profiles of the original carbon (X1) and several oxidized materials.

or strong oxidation conditions, the original porous texture, particle morphology and structural order is preserved.

The chemical evolution, at both bulk and surface levels, was studied by means of elemental analysis, temperature programmed desorption (TPD) and X-ray photoelectron spectroscopy (XPS) techniques. The elemental contents obtained from elemental analysis and XPS, expressed as weight percentage, are collected in Table 2. The O/C ratio is also included to provide an estimate for the oxidation degree of the samples. Results obtained from both techniques are very similar to each other, indicating that the used oxidants modify both the surface and the bulk of the materials. As expected, the oxygen content, and therefore the oxidation degree of the carbons, increases with both oxidizing agent concentration and treatment time (although the former seems to have a greater effect), and reaches a maximum value around 9 wt.% for OMCs treated with 5 M and 14.55 M HNO_3 at 80 °C and room temperature.

The amount and type of oxygen functional groups introduced after the oxidation process were determined by TPD and XPS. In the interpretation of TPD measurements we assume that each type of oxygen-containing group decomposes giving rise to CO and/or CO_2 moieties at different temperatures. The deconvolution of CO and CO_2 profiles into single peaks (using multiple Gaussian functions) leads to the determination of the specific functional groups.

TPD profiles of several samples are recorded in Figs. 4 and 5. As one can see in these figures, the original carbon (X1) shows CO evolution, but does not show any CO_2 evolution. This is an indication that X1 carbon contains oxygenated functional groups that are desorbed as CO, and its low amount (804.5 μmol g^{-1}, see Table 3) indicates a low functionalization degree. The OMCs oxidized under mild conditions (H_2O_2 and 0.5 M HNO_3) yield CO profiles with a high number of peaks in the entire range of temperature. Comparing with the CO profile corresponding to X1 sample, a higher CO evolution is mainly observed between 600 and 700 °C when oxidation is carried out with H_2O_2; if oxidation is performed with 0.5 M HNO_3, in the CO evolution there are increments between 600 and 700 °C, and above 850 °C.

Using HNO_3 concentrations higher than 0.5 M (i.e. 2, 5 and 14.55 M HNO_3), or longer treatment time for a given concentration, CO desorption between 600 and 700 °C becomes clearly predominant and, additionally, the number of peaks decreases.

Deconvolution of the CO profiles corresponding to the raw material (X1) and oxidized carbon X1oxC/1 are shown in Fig. 6 as representative examples. The deconvolution of other CO profiles is given in Fig. S2 at Supporting Information. Several peaks between 250 and 500 °C are distinguished and could be assigned to the desorption of carboxylic anhydrides in different chemical environments [26] in the case of the oxidized samples, as it will be explained later. However, the shoulders at low temperatures present in the CO spectra of the X1 sample (the three small peaks at lower temperature shown in Fig. 6) cannot be justified by the desorption of carboxylic anhydride groups because this functional group decomposes by releasing both CO and CO_2, and no CO_2 evolution is observed in this carbon. Moreno-Castilla et al. [27], based in the work of Surygala et al. [28], assigned the CO peaks at low temperature to the decomposition of carbonyl groups in

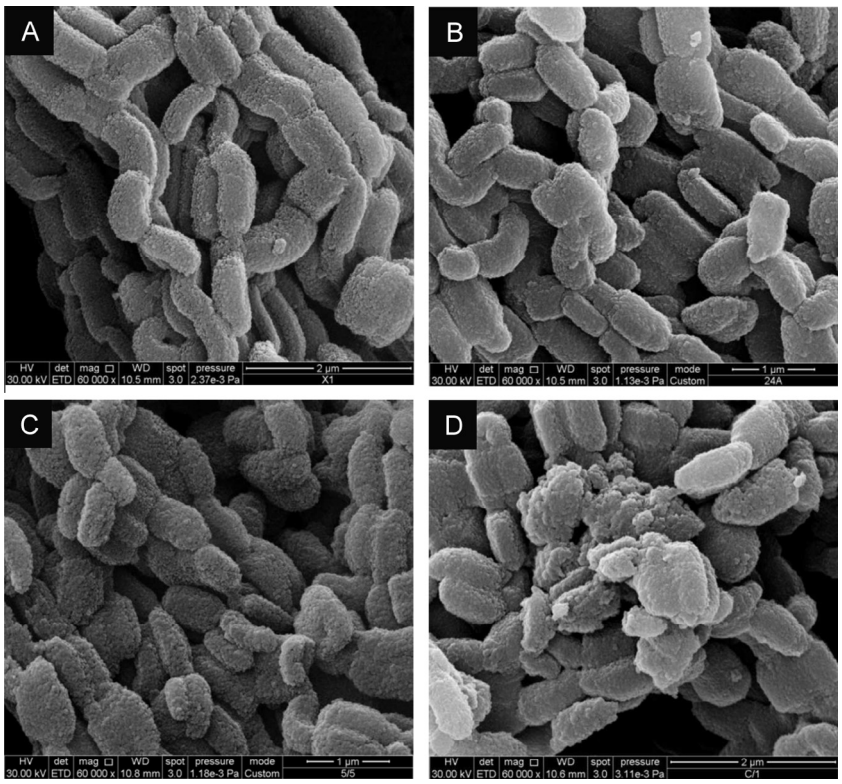

Fig. 3 – SEM micrographs of (A) raw carbon and some carbons obtained through different strength oxidation treatments: (B) 30% (v/v) H_2O_2/room temperature/24 h, (C) 5 M HNO_3/80 °C/5 h and (D) 14.55 M HNO_3/room temperature/1 h; the latter shows an isolated damaged area, but the global structure of this oxidized carbon is the same as that of the starting material.

Table 2 – Elemental analysis and XPS results for raw and oxidized carbon materials.

Sample	Elemental analysis (wt.%)					XPS (wt.%)		
	C	H	N	O	O/C	C	O	O/C
X1	97.5	0.2	0.0	2.2	0.02	97.0	3.0	0.03
X1ox4A	96.7	0.6	0.0	2.7	0.03	97.2	2.8	0.03
X1ox24A	96.4	0.6	0.0	2.7	0.03	95.4	4.6	0.05
X1ox0.5/1	97.7	0.2	0.0	2.1	0.02	97.4	2.7	0.03
X1ox0.5/3	97.4	0.2	0.0	2.5	0.03	97.3	2.7	0.03
X1ox0.5/5	95.0	0.1	0.2	4.6	0.05	94.4	5.6	0.06
X1ox2/1	94.5	0.2	0.3	5.0	0.05	94.3	6.1	0.06
X1ox2/3	93.1	0.2	0.3	6.4	0.07	93.6	6.5	0.07
X1ox2/5	92.9	0.2	0.3	6.7	0.07	93.0	7.0	0.07
X1ox5/3	90.4	0.4	0.4	8.9	0.10	91.8	8.2	0.09
X1ox5/5	90.4	0.3	0.2	9.1	0.10	91.1	8.9	0.10
X1oxC/1	90.7	0.3	0.1	8.9	0.10	91.4	8.6	0.09

α-substituted ketones and aldehydes. In a recent work, Li et al. [29] observed the evolution of CO together with H_2O at the same low temperature range, and they assigned these low-temperature CO peaks to the decomposition of carboxyl groups into CO and H_2O. However, in the case of X1 sample this low-temperature evolution of CO cannot be assigned to carboxylic groups because, as mentioned above, it presents no CO_2 evolution; for these reasons, it could be assigned to α-substituted carbonyls in ketone and aldehyde functional groups. Peaks between 600 and 700 °C, whose intensity increases dramatically as the oxidation becomes increasingly severe, can be assigned to the desorption of ethers, phenols and hydroquinones also in different chemical environments; and finally, peaks above 850 °C can be assigned to carbonyl, quinone and semiquinone groups [12,30–34]. Another peak around 1000 °C (the CO profile does not return to the base line above 1000 °C) was used for deconvolution, but it was not taken into account for the quantitative analysis; it could be assigned to basic groups, such as a pyrones and chromenes [35,39].

As concerns the CO_2 profiles (Fig. 5), and as noted before, it is clearly observed the appearance of peaks related to oxygen

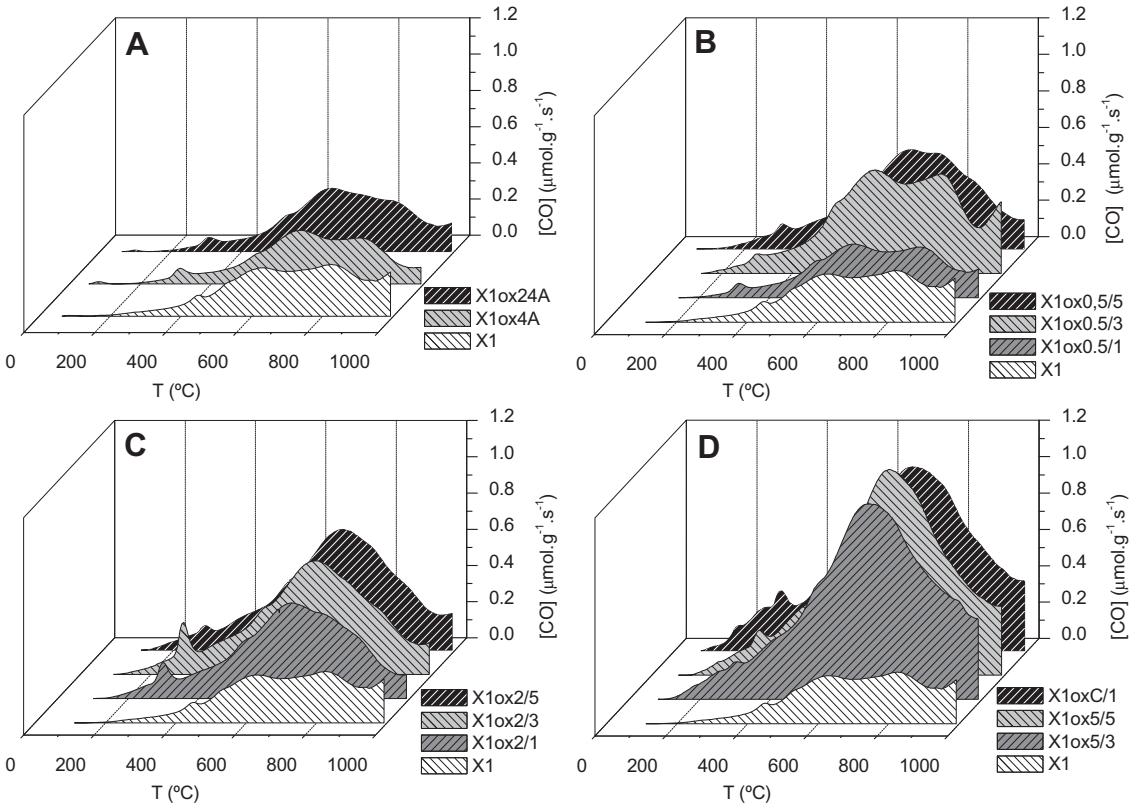

Fig. 4 – CO profiles of raw carbon (X1) and oxidized materials: (A) 30% (v/v) H_2O_2, (B) 0.5 M HNO_3, (C) 2 M HNO_3 and (D) 5 M and 14.55 M HNO_3.

functional groups, mainly acidic, even after mild oxidation treatments with hydrogen peroxide and nitric acid; their area increases with increasing oxidant concentration and oxidation time. When H_2O_2 is used as oxidizing agent, longer treatments mainly produce an increase in the area of peaks between 200 and 300 °C (strong carboxylic acids), but to a lower extent than when using 0.5 M HNO_3 (compare Fig. 5A and B). When the oxidation is carried out with higher concentrations of nitric acid (2, 5 and 14.55 M) and longer oxidation times, a great evolution of CO_2 is observed between 250 and 400 °C (weakly carboxylic acids), and the highest CO_2 peak areas are obtained for the sample oxidized with concentrated 14.55 M HNO_3 (compare Fig. 5C and D).

Deconvolution of the CO_2 profile for X1oxC/1 sample is shown in Fig. 7. Other deconvoluted profiles can be found in Fig. S3 at Supporting Information. Different peaks can be distinguished. The two small peaks (and probably a third one that is contained in the maximum of the large peak at 250 °C) correlate with the small peaks desorbed at temperatures lower than 350 °C that appear in the CO profile of this sample. Their positions and areas are almost the same, and for this reason they could be assigned to the desorption of carboxylic anhydrides in different chemical environments. The same correlation exists between the two peaks with higher areas located from 400 to 510 °C in the CO_2 profile and the corresponding peaks in the CO profile, and therefore they can also be assigned to carboxylic anhydrides in different chemical environments. The intense peak at ~250 °C could be due to the desorption of carboxylic acids and finally, the peaks that appear above 600 °C are due to lactones and lactols [12,30–34].

Globally considered, the TPD results indicate that oxidation of OMCs by means of H_2O_2 mainly introduces phenols and hydroquinones, and their concentration increases with the treatment time; through nitric acid oxidation under mild conditions, phenols, hydroquinones and carboxylic acids are mostly generated, their quantity being enhanced at higher nitric acid concentration and oxidation time.

The XPS technique is often used to identify the nature of chemical bondings in carbon material surfaces. In this way, the deconvolution of C1s and O1s high-resolution spectra provides useful information on the nature of the oxygen functional groups generated on the carbon surface. Thus, TPD and XPS techniques give complementary results to characterize the chemical evolution of the original OMC with oxidation treatments. XPS high-resolution spectra of the starting and oxidized carbons were also deconvoluted into single peaks (recorded in Fig. 8), and each peak was assigned to a certain type of chemical bonding. As expected, the main element at the surface was carbon, and its concentration decreased with increasing oxygen content when higher oxidant concentration and treatment times were used. Moreover, on the surface of all samples no elements other than carbon and oxygen were found.

The relatively low oxygen concentration at the surface of the starting material indicates that this is well ordered and with a low concentration of defects [2]. Deconvolution of its C1s high-resolution spectrum (Fig. 8A) gives rise to six peaks

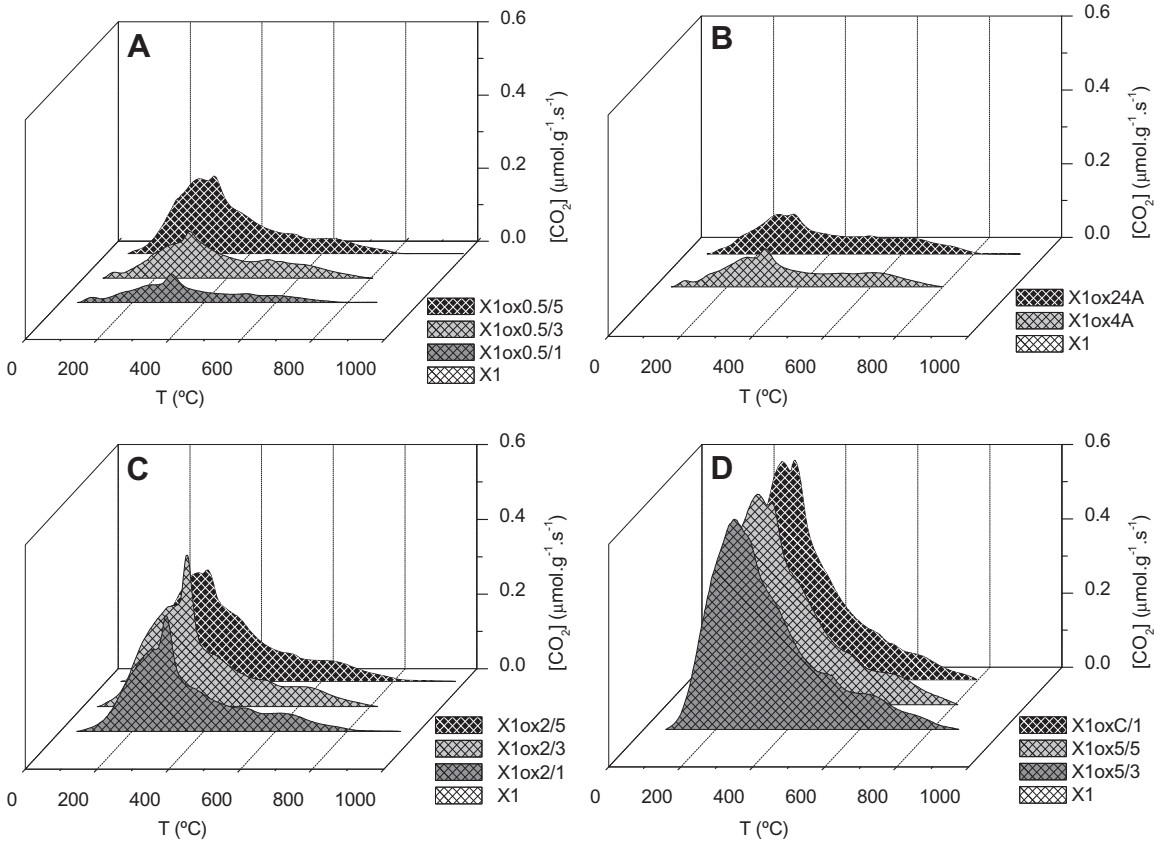

Fig. 5 – CO_2 profiles of raw carbon (X1) and oxidized materials: (A) 0.5 M HNO_3, (B) 30% (v/v) H_2O_2, (C) 2 M HNO_3 and (D) 5 M and 14.55 M HNO_3.

indicating the presence of graphitic Csp^2 at 284.39 eV, C–O and C–OH carbon species of alcohol and ether groups at 285.39 eV, C-=O bonds in carbonyl groups at 286.69 eV, carboxyl and ester functional groups at 289.09 eV, and finally, $\Pi \rightarrow \Pi^*$ transitions in highly ordered and graphitic structures at 291.39 eV. The O1s high-resolution spectrum (Fig. 8A) consists of a broad peak with low intensity; the deconvolution of O1s envelope gives three peaks: a first one at 531.8 eV, due possibly to the presence of C-=O in quinones, a second peak at 533.2 eV assigned to oxygen in phenols, non-carbonyl oxygen in carboxyls and lactones, and a contribution of single-bonded oxygen in alcohol and ether groups; and a third and small peak at 535.4 eV, which is attributed to chemisorbed/physisorbed water [2,18,32,37].

With increasing oxidant concentration and treatment times, the oxygen content and the number of peaks related to different surface oxygen functional groups increase. Broad peaks indicate the existence of different chemical states of oxygen [35,36,38]. In this way, in the sample oxidized with H_2O_2 for 24 h at room temperature (Fig. 8B), the C1s high-resolution spectrum comprises six peaks, being very similar to the starting material spectrum with the only difference that an increase in the relative intensity of the peak at 285.36 eV is produced, which is ascribable to generation of alcohol and ether groups.

Larger differences are observed in the O1s spectrum (Fig. 8B), in which the signal is considerably stronger. This spectrum presents a good fit with three peaks: two of them with similar intensities at 531.88 and 533.30 eV, assigned to C-=O bonds in esters, anhydrides and carboxyls, and single-bonded oxygen in ether and ester groups, respectively. A weak peak at 535.78 eV indicates the presence of chemisorbed water on this material surface [2,38–40].

When oxidation is carried out with 0.5 M HNO_3, C1s and O1s spectra (Fig. 8C) with stronger differences regarding the X1 spectrum are obtained; here, the C1s spectrum can be fitted to six peaks too, but the areas of the peaks at 285.33, 286.63 and 289.03 eV are higher indicating the generation of greater amounts of alcohol and ether groups, carbonyl and carboxyl groups, respectively. The O1s spectrum was fitted to three peaks, but displaying some differences with respect to the H_2O_2 treatment, too. These differences include a shift of the peak located at 532.04 eV towards higher bonding energies than the corresponding one in H_2O_2. This peak is very broad and may include several bonds, among them, C-=O in esters and anhydrides, and C–O in alcohol and ether groups, whose concentration is slightly higher than that obtained with H_2O_2 during 24 h of treatment. Moreover, this peak is predominant in area over the second one, located at 533.26 eV, and assigned to singly-bonded oxygen in ether and anhydride groups, indicating a foreground generation of these functional groups. The third peak, at 534.80 eV, is shifted to lower bonding energies, and is related to C–OH bondings in carboxylic acids [2,38,39]. Its area is slightly greater

Table 3 – CO and CO_2 concentrations (μmol g^{-1}) obtained in the TPD experiments.

Sample	[CO]	[CO_2]
X1	805	–
X1ox4A	732	175
X1ox24A	866	215
X1ox0.5/1	797	113
X1ox0.5/3	1586	211
X1ox0.5/5	1384	346
X1ox2/1	1326	384
X1ox2/3	1540	480
X1ox2/5	1596	488
X1ox5/3	2771	963
X1ox5/5	2762	935
X1oxC/1	2768	963

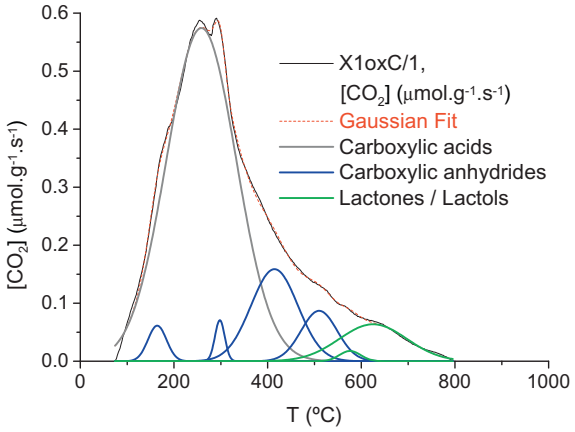

Fig. 7 – CO_2 profile deconvolution of oxidized carbon using 14.55 M HNO_3/room temperature/1 h (X1oxC/1).

than following the H_2O_2 treatment, being in agreement with TPD results shown above. Therefore, XPS spectra of 0.5 M HNO_3/5 h/80 °C-treated sample indicate the presence of higher amounts of carboxylic acids and alcohol/anhydride groups than for the carbon oxidized with H_2O_2/24 h/room temperature.

Finally, the samples treated with 5 M and 14.55 M HNO_3 (Fig. 8D and E, respectively) show C1s high-resolution spectra very similar to each other, and very different from those corresponding to milder oxidation treatments. For the last two, the XPS profiles could be fitted to six peaks, with very similar width and area values, thus indicating the similarity of their surface carbon bondings. This seems reasonable, since their carbon and oxygen mass percentages are in the same range and the TPD results showed occurrence of almost the same oxygen functional groups. The main C1s peak in both samples is placed at 284.34 eV, being assigned to highly delocalized Csp^2 bondings; the second peak, at 285.34 eV, is broader than in the previous cases, indicating the presence of greater amounts of defects on the material surface. The rest of the peaks are practically the same as those mentioned above for samples treated under milder oxidant conditions. However, interesting conclusions can be drawn when studying the corresponding O1s high-resolution spectra, which were fitted to three peaks at 531.6 ± 0.2, 533.1 ± 0.13 and 534.6 ± 0.16 eV. The most important features are the differences between the relative areas and widths of the two peaks located at lower bonding energies. Thus, in X1ox5/5 sample the first peak has higher area and is broader than the second one, and the opposite is observed in X1oxC/1 sample. Broad peaks point to the presence of different oxygen chemical states, and in both samples this is explained by the contribution of C–OH linkages in carboxylic functional groups [38–40]. This is confirmed by the fact that the first peak in sample X1ox5/5 and the first and second peaks in X1oxC/1 sample are shifted to lower bonding energies with respect to carbons treated under mild conditions.

Summarizing, when carbon is oxidized with hydrogen peroxide mainly phenols and hydroquinones are generated, but in lower amounts than using low concentration of nitric acid. Mild oxidation with nitric acid generates a wide range of functional groups. Finally, phenols, hydroquinones, anhydrides and carboxylic acids are predominantly introduced using higher concentrations of HNO_3.

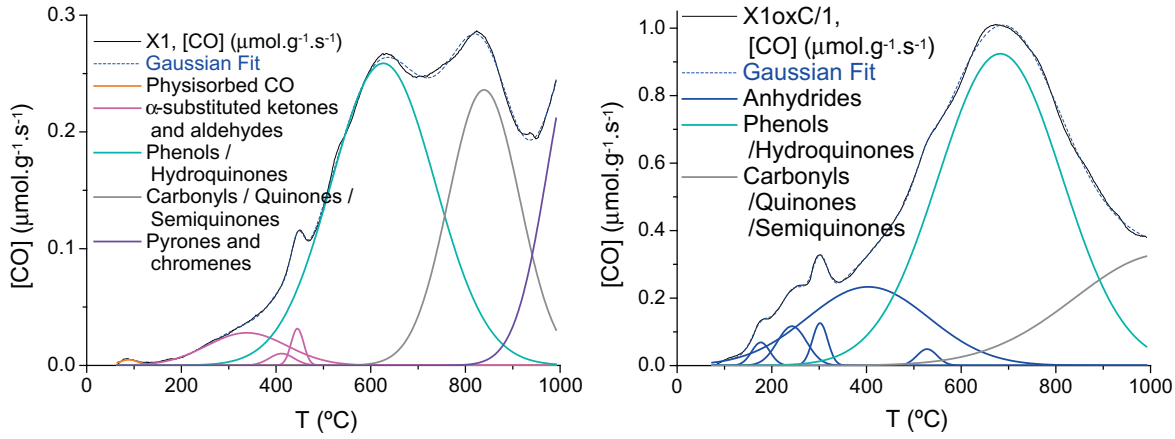

Fig. 6 – CO profile deconvolution of original carbon (X1) and the material oxidized with 14.55 M HNO_3/room temperature/1 h (X1oxC/1).

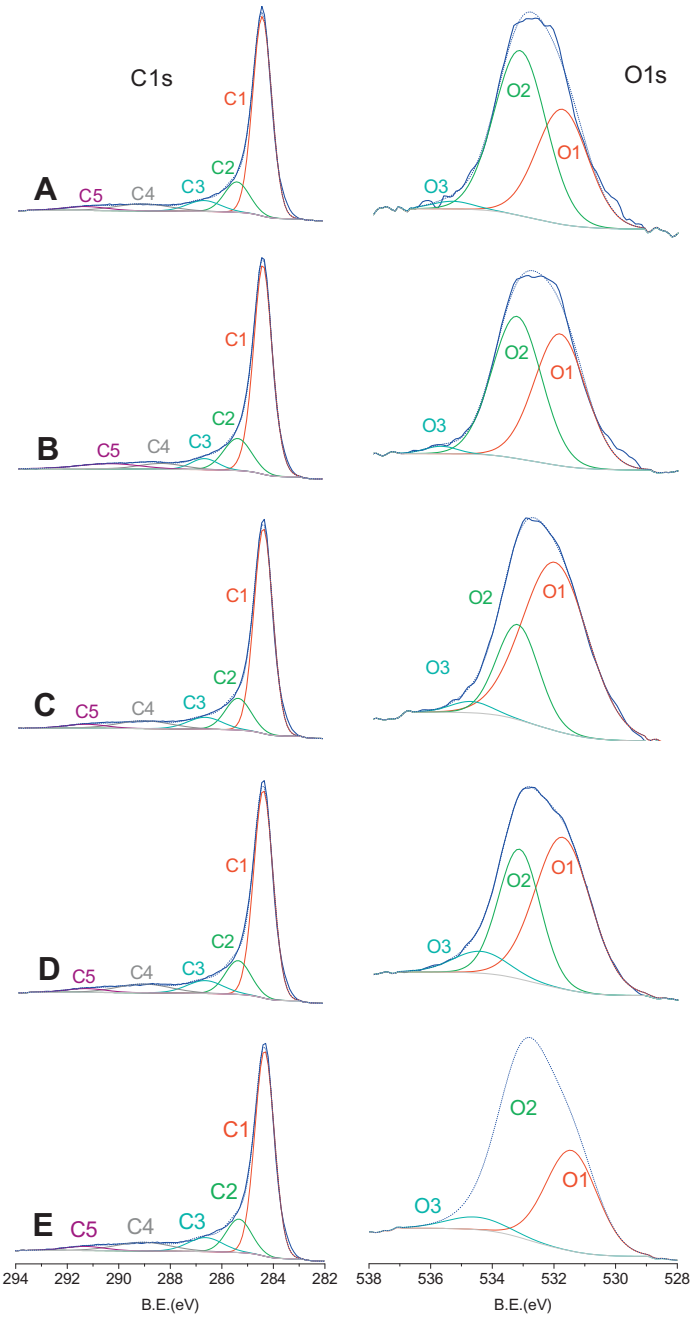

Fig. 8 – C1s and O1s high-resolution spectra of mesoporous carbons: (A) X1, (B) X1ox24A, (C) X1ox0.5/5, (D) X1ox5/5 and (E) X1oxC/1.

4. Conclusions

Through different oxidation treatments with nitric acid and hydrogen peroxide, it was possible to introduce a high variety of oxygen functional groups at the surface of an OMC. By changing the nature and concentration of the oxidizing agent and the treatment time it is possible to introduce different amounts and types of oxygen-containing functional groups, without altering neither the structural arrangement nor the porous texture of the starting OMC, even under severe oxidizing conditions. Although the original carbon is resistant to oxidative treatments, through the most severe oxidation treatments with nitric acid it is possible to introduce up to 9 wt.% oxygen on the surface, mainly in the form of carboxylic, phenol and hydroquinone functional groups. When oxidation is carried out with hydrogen peroxide at room temperature, only 3 wt.% of oxygen is incorporated, mainly by formation of phenolic groups and hydroquinones.

Appendix A. Supplementary data

Supplementary data associated with this article can be found, in the online version, at http://dx.doi.org/10.1016/j.carbon.2013.06.011.

REFERENCES

[1] Ryoo R, Joo SH, Kruk M, Jaroniec M. Ordered mesoporous carbons. Adv Mater 2001;13(9):677–81.
[2] Darmstadt H, Roy C, Kaliaguine S, Choi SJ, Ryoo R. Surface chemistry of ordered mesoporous carbons. Carbon 2002;40(14):2673–83.
[3] Choy KL. Chemical vapour deposition of coatings. Prog Mater Sci 2003;48(2):57–170.
[4] Parmentier J, Saadhallah S, Reda M, Gibot P, Roux M, Vidal L, et al. New carbons with controlled nanoporosity obtained by nanocasting using a SBA-15 mesoporous silica host matrix and different preparation routes. J Phys Chem Solids 2004;65(2–3):139–46.
[5] Radovic LR, Moreno-Castilla C, Rivera-Utrilla J. Carbon materials as adsorbents in aqueous solutions. Chemistry and physics of carbon, vol. 27. New York: Dekker; 2001. p. 227–382.
[6] Stein A, Wang Z, Fierke MA. Functionalization of porous carbon materials with designed pore architecture. Adv Mater 2009;21(3):265–93.
[7] Moreno-Castilla C, López-Ramón MV, Carrasco-Marín F. Changes in surface chemistry of activated carbons by wet oxidation. Carbon 2000;38(14):1995–2001.
[8] Pradhan BK, Sandle NK. Effect of different oxidizing agent treatments on the surface properties of activated carbons. Carbon 1999;37(8):1323–32.
[9] Jaramillo J, Álvarez PM, Gómez-Serrano V. Oxidation of activated carbon by dry and wet methods: surface chemistry and textural modifications. Fuel Process Technol 2010;91(11):1768–75.
[10] Bazula PA, Lu A-H, Nitz J-J, Schüth F. Surface and pore structure modification of ordered mesoporous carbons via a chemical oxidation approach. Microp Mesop Mater 2008;108(1–3):266–75.
[11] Li H, Xi H, Zhu S, Wen Z, Wang R. Preparation, structural characterization and electrochemical properties of chemically modified mesoporous carbon. Microp Mesop Mater 2006;96(1–3):357–62.
[12] Lázaro MJ, Calvillo L, Bordejé EG, Moliner R, Juan R, Ruiz CR. Functionalization of ordered mesoporous carbons synthesized with SBA-15 silica as template. Microp Mesop Mater 2007;103(1–3):158–65.
[13] Lu A-H, Li W-C, Muratova N, Spliethoff B, Schuth F. Evidence for C–C bond cleavage by H_2O_2 in a mesoporous CMK-5 type carbon at room temperature. Chem Commun 2005;0(41):5184–6.
[14] Vinu A, Hossian KZ, Srinivasu P, Miyahara M, Anandan S, Gokulakrishnan N, et al. Carboxy-mesoporous carbon and its excellent adsorption capability for proteins. J Mater Chem 2007;17(18):1819–25.
[15] Jun S, Joo SH, Ryoo R, Kruk M, Jaroniec M, Liu Z, et al. Synthesis of new, nanoporous carbon with hexagonally ordered mesostructure. J Am Chem Soc 2000;122(43):10712–3.
[16] Kruk M, Jaroniec M, Kim T-W, Ryoo R. Synthesis and characterization of hexagonally ordered carbon nanopipes. Chem Mater 2003;15(14):2815–23.
[17] Vinu A, Srinivasu P, Takahashi M, Mori T, Balasubramanian VV, Ariga K. Controlling the textural parameters of mesoporous carbon materials. Microp Mesop Mater 2007;100(1–3):20–6.
[18] Wang D-W, Li F, Liu M, Cheng H-M. Improved capacitance of SBA-15 mesoporous carbons after modification with nitric acid oxidation. New Carbon Mater 2007;22(4):307–14.
[19] Kim T-W, Park I-S, Ryoo R. A synthetic route to ordered mesoporous carbon materials with graphitic pore walls. Angew Chem 2003;115(36):4511–5.
[20] Joo SH, Choi SJ, Oh I, Kwak J, Liu Z, Terasaki O, et al. Ordered nanoporous arrays of carbon supporting high dispersions of platinum nanoparticles. Nature 2001;412(6843):169–72.
[21] Su F, Zeng J, Bao X, Yu Y, Lee JY, Zhao XS. Preparation and characterization of highly ordered graphitic mesoporous carbon as a Pt catalyst support for direct methanol fuel cell. Chem Mater 2005;17(15):3960–7.
[22] Zhao D, Feng J, Huo Q, Melosh N, Freidckson GH, Chmelka BF, et al. Triblock copolymer synthesis of mesoporous silica with periodic 50 to 300 Angstrom pores. Science 1998;279(5350):548–52.
[23] Enterría M, Suárez-García F, Martínez-Alonso A, Tascón JMD. Synthesis of ordered micro–mesoporous carbons by activation of SBA-15 carbon replicas. Microp Mesop Mater 2012;151:390–6.
[24] Lee J-S, Joo SH, Ryoo R. Synthesis of mesoporous silicas of controlled pore wall thickness and their replication to ordered nanoporous carbons with various pore diameters. J Am Chem Soc 2002;124(7):1156–7.
[25] Kruk M, Jaroniec M, Sakamoto Y, Terasaki O, Ryoo R, Ko CH. Determination of pore size and pore wall structure of MCM-41 by using nitrogen adsorption, transmission electron microscopy, and X-ray diffraction. J Phys Chem B 2000;104(2):292–301.
[26] Szymanski GS, Karpinski Z, Biniak S, Swiatkowski A. The effect of the gradual thermal decomposition of surface oxygen species on the chemical and catalytic properties of oxidized activated carbons. Carbon 2002;40(14):2627–39.
[27] Moreno-Castilla C, Carrasco-Marín F, Mueden A. The creation of acid carbon surfaces by treatment with $(NH_4)_2S_2O_8$. Carbon 1997;35(10–11):1619–26.
[28] Surygala J, Wandas R, Sliwka E. Oxygen elimination in the process of non-catalytic liquefaction of brown coal. Fuel 1993;72(3):409–11.
[29] Li N, Ma X, Zha Q, Kim K, Chen Y, Song C. Maximizing the number of oxygen-containing functional groups on activated carbon by using ammonium persulfate and improving the temperature-programmed desorption characterization of carbon surface chemistry. Carbon 2011;49(15):5002–13.
[30] Machado BF, Gomes HT, Serp P, Kalck P, Figueiredo JL, Faria JL. Carbon xerogel supported noble metal catalysts for fine chemical applications. Catal Today 2010;149(3–4):358–64.
[31] Pereira MFR, Soares SF, Órfao JJM, Figueiredo JL. Adsorption of dyes on activated carbons: influence of surface chemical groups. Carbon 2003;41(4):811–21.
[32] Vinke P, Van Der Eijk M, Verbree M, Voskamp AF, Van Bekkum H. Modification of the surface chemistry of a gas-activated carbon and a chemically activated carbon with nitric acid, hypochlorite, and ammonia. Carbon 1994;32(4):675–86.
[33] Calvillo L, Moliner R, Lázaro MJ. Modification of the surface chemistry of mesoporous carbons obtained through colloidal silica templates. Mater Chem Phys 2009;118(1):249–53.
[34] Gomes HT, Miranda SM, Sampaio MJ, Silva AMT, Faria JL. Activated carbons treated with sulphuric acid: catalysts for catalytic wet peroxide oxidation. Catal Today 2010;151(1–2):153–8.
[35] Zielke U, Huttinger KJ, Hoffman WP. Surface-oxidized carbon fibers: I. Surface structure and chemistry. Carbon 1996;34(8):983–98.
[36] Weidenthaler C, Lu A-H, Schmidt W, Schüth F. X-ray photoelectron spectroscopic studies of PAN-based ordered mesoporous carbons (OMC). Microp Mesop Mater 2006;88(1–3):238–43.
[37] Polzonetti G, Lucci G, Altamura P, Ferri A, Paolucci G, Goldoni A, et al. Thiophene-containing organometallic polymers

studied by near-edge X-ray absorption spectroscopy. Surf Interface Anal 2002;34(1):588–92.
[38] Dongil AB, Bachiller-Baeza B, Guerrero-Ruiz A, Rodríguez-Ramos I, Martínez-Alonso A, Tascón JMD. Surface chemical modifications induced on high surface area graphite and carbon nanofibers using different oxidation and functionalization treatments. J Colloid Interface Sci 2011;355(1):179–89.
[39] Boudou JP, Paredes JI, Cuesta A, Martínez-Alonso A, Tascón JMD. Oxygen plasma modification of pitch-based isotropic carbon fibres. Carbon 2003;41(1):41–56.
[40] Seredych M, Hulicova-Jurcakova D, Lu GQ, Bandosz TJ. Surface functional groups of carbons and the effect on their chemical character, density and accessibility to ions on electrochemical performance. Carbon 2008;46(11):1475–88.